BUTTERWORTH HEINEMANN

Polymer Vol. 36 No. 13, pp. 2597–2601, 1995

0032-3861/95/$10.00 + 0.00

Possibility of porosity control in nylon-6 membranes

Nobuyuki Tanaka
Department of Biological and Chemical Engineering, Faculty of Engineering, Gunma University, Kiryu 376, Japan
(Received 4 August 1994; revised 23 January 1995)

The possibility of porosity control in nylon-6 membranes was investigated. By adding water onto the surface of a concentrated nylon-6 solution in calcium chloride–methanol mixture in a cylindrical glass bottle, a three-phase structure of solid, gel and solution (in order from the top) appeared. The thickness of the gel phase was 2.5–4 mm and became larger as the time elapsed after adding water. The interfaces between solid and gel, and between gel and solution, shifted downwards at very slow rates, 0.224 and 0.263 mm h^{-1} at 20°C, respectively. In the gel, the behaviour of pore growth was observed in real time. The membranes have spherical pores with a pore size distribution, and the pore size increases with increasing preparation temperature. On the basis of these observations, a schematic process of membrane formation was proposed as a fundamental of porosity control.

(Keywords: nylon-6 membrane; phase inversion; porosity control)

INTRODUCTION

Polyamide solutions in calcium chloride–methanol mixtures are well known as casting solutions for the preparation of membranes[1–5]. The structure and properties of the membrane may originate from the character of the solution: a dilute solution of nylon-6 (N6) in a mixture of 15 g $CaCl_2$ and 100 ml CH_3OH is even a theta solution[6] in spite of the influence of ions. For a concentrated solution of N6 in this mixture, by adding water onto the solution surface, a three-phase structure of solid, gel and solution (in order from the top) has been observed[7,8] (see *Figure 1*). In particular, the behaviours of sol–gel and gel–solid inversions and pore growth in the gel were observed visually in real time[8]. In this case, water is the non-solvent pore former. The membrane prepared is a typical phase inversion membrane[9] and has a pore size distribution of spherical pores, with the larger pores in the lower parts of the membrane[8]. Accordingly, if a functional ultra-thin membrane is coated on the surface of this membrane, the original membrane is regarded as the supporting layer (membrane) of the ultra-thin membrane in a composite membrane[10]. Polysulfone containing acidic and basic groups is a typical material for supporting membranes[10] with larger pores in the lower parts. In this paper, on the basis of these observations for N6, a schematic process of membrane formation is simulated as a fundamental of porosity control. In general[9,10], the porosity of membranes should be controlled by the non-solvent concentration in the casting solution and the preparation temperature.

EXPERIMENTAL

Casting solution and gelation

N6 solutions in calcium chloride–methanol mixtures (6.67 and 8.33 g N6/20 g $CaCl_2$/100 ml CH_3OH) were selected as suitable casting solutions for preparing membranes. The casting solution was concentrated naturally by leaving it open to the atmosphere in a cylindrical glass bottle (30 mm diameter) in a room at about 20°C and 80% r.h. until a skin formed on the solution surface. Then, after putting the bottle in an incubator controlled at a constant temperature (10, 20 and 30°C), water was added onto the surface skin. The solution after adding water showed gelation behaviour, as shown in *Figure 2*. For

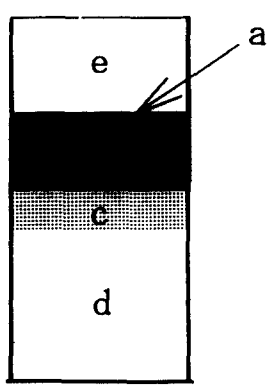

Figure 1 Schematic diagram of pore formation process: (a) surface skin, (b) solid, (c) gel, (d) solution and (e) water

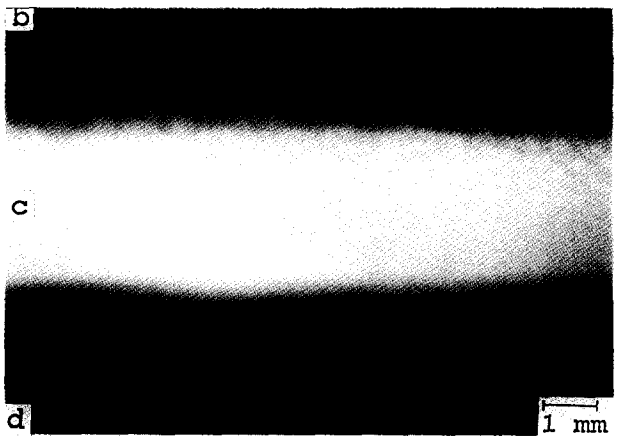

Figure 2 Photograph of pore formation process at 20°C for a solution of 6.67 g N6/20 g $CaCl_2$/100 ml CH_3OH. The thickness of the gel phase is about 3 mm; (b) solid, (c) gel and (d) solution

solutions with a lower concentration of N6 (1.67 or 3.33 g N6/20 g $CaCl_2$/100 ml CH_3OH) and a higher concentration of N6 (11.7 g N6/20 g $CaCl_2$/100 ml CH_3OH), gelation behaviour was not observed and a membrane could not be prepared. For solutions of 5.00 or 10.0 g N6/20 g $CaCl_2$/100 ml CH_3OH, useful membranes to investigate the possibility of porosity control could not be prepared, though gelation behaviour was observed. The gelation and solidification rates, and the rates of downwards shift of the interfaces between solution and gel, and between gel and solid, were measured by a cathetometer from the outside through the transparent plastic door of the incubator. The membranes prepared via these processes were washed sufficiently with water and then dried under room conditions before being photographed.

Photography

The pictures (*Figures 2–4*, *7* and *8*) of the porous morphology and the gelation behaviour were taken by a camera with a bellows focusing attachment.

Titration of solidification

The titration of solidification by water was carried out for six solutions (1.67, 3.33, 5.00, 6.67, 8.33 and 10.0 g N6/20 g $CaCl_2$/100 ml CH_3OH) in a room kept at constant temperature (20 or 30°C). Water was added drop by drop into a stirred solution using a pipette. The solidification curves at 20 and 30°C in *Figure 9* show the amount of water added until 10 g of the solution changes to a state like bean curd suddenly in the course of titration for four solutions (5.00, 6.67, 8.33 and 10.0 g N6/20 g $CaCl_2$/100 ml CH_3OH), and is apparently separated into a liquid and solidified flakes for the other solutions (1.67 and 3.33 g N6/20 g $CaCl_2$/100 ml CH_3OH), in which a state like bean curd did not occur.

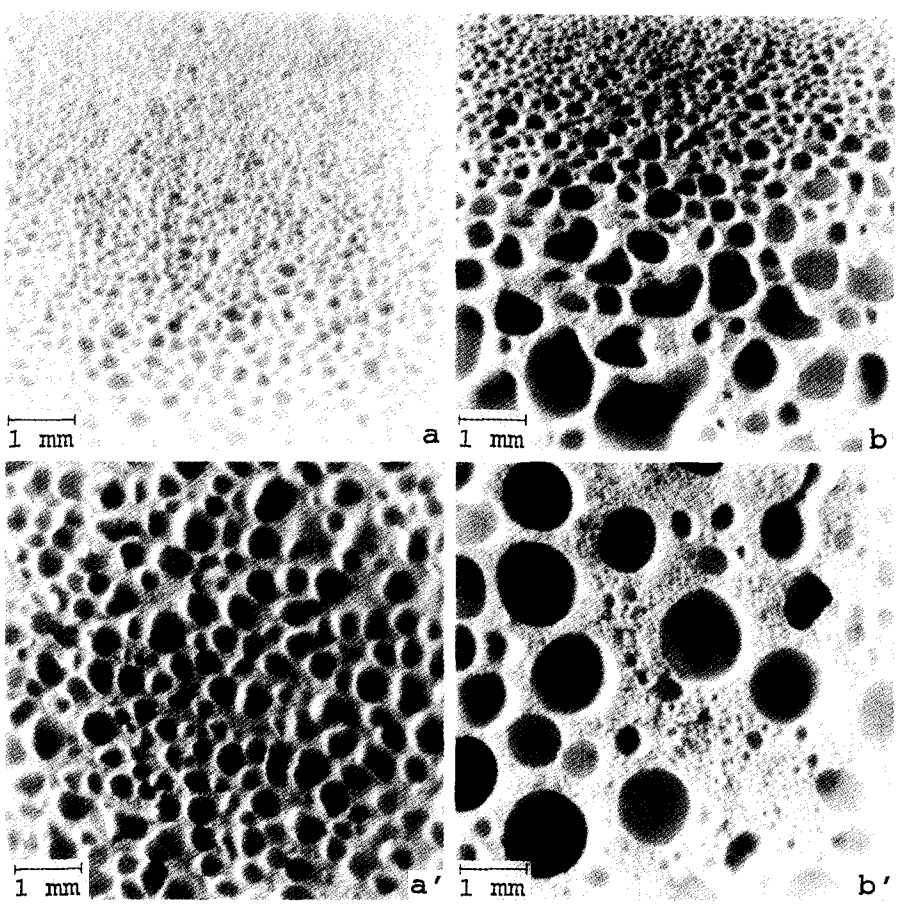

Figure 3 Sectional morphology for N6 membranes prepared from a solution of 6.67 g N6/20 g $CaCl_2$/100 ml CH_3OH at 10°C (a, a′) and 30°C (b, b′). (a, b) Vertical sections. The lower parts have larger pores. (a′, b′) Horizontal cross-sections in the lower parts, which were formed about a week after adding water

RESULTS AND DISCUSSION

Pore formation

Figure 1 shows a schematic diagram of the pore formation process after adding water onto the surface skin (a). In *Figure 1*, three phases of solid (b), gel (c) and solution (d) are shown in order from the top. The thickness of the gel phase at 20°C was 2.5–4 mm, 2–4 mm and 1 mm for solutions of 6.67, 8.33 and 10.0 g N6/20 g $CaCl_2$/100 ml CH_3OH, respectively, and became larger with the elapsed time after adding water, except for the solution of 10.0 g N6/20 g $CaCl_2$/100 ml CH_3OH. The observations and discussion here are for a solution of 6.67 g N6/20 g $CaCl_2$/100 ml CH_3OH. The interfaces between solid and gel, and between gel and solution, shifted downwards at very slow rates, 0.224 and 0.263 mm h^{-1} at 20°C, respectively. In *Figure 2* an actual photograph of pore formation at 20°C is shown; the behaviours of sol–gel and gel–solid inversions and pore growth in the gel could be observed visually. In the gel region near the solid phase, pores of spherical shape are observed. *Figure 3* shows the sectional morphology for N6 membranes prepared at 10 and 30°C. The membranes have a distribution of spherical pore size, and with increasing preparation temperature, the pore size increases. The lower parts of a membrane have larger pores. This result may be attributed to the decrease of the concentration of N6 in the solution phase (d in *Figure 1*) with the progress of gelation and solidification[11]. *Figure 4* shows the morphology of vertical sections for N6 membranes prepared from solutions of 6.67 and 8.33 g N6/20 g $CaCl_2$/100 ml CH_3OH at 20°C. The pore size decreases with increasing concentration of N6 in the casting solution. *Figure 5* shows the relationships between $-\ln G$ and $1/T$ for sol–gel and gel–solid inversions. In the temperature range of 10–35°C, a straight line was obtained for each inversion, where G is the gelation or solidification rate (cm h^{-1}) and T is the absolute temperature (K).

Schematic process of membrane formation

In *Figure 6*, the amounts of additional water per unit volume needed for solidification (α), sol–gel inversion (β) and phase separation (γ) at a horizontal cross-section point are shown schematically as functions of the concentration of N6 in the calcium chloride–methanol mixture, respectively. The schematic process of membrane formation in *Figure 6* is as follows: First, water is added onto a concentrated solution with a surface skin at point A or A′. Water diffuses into the solution through the surface skin. Here, let us focus on the inversion behaviours in a very small constant volume of a horizontal cross-section point at a fixed site of the glass bottle.

For a solution at point A′. The increase of water into the phase separation region over a point Q′ on the curve γ results in liquid–liquid phase separation. The concentration of N6 in the N6-rich phase increases with increasing amount of water. At point R, the N6-rich phase is gelled. With increasing water, the separated gel phase increases the concentration of N6 along the curve γ, accompanied by pore growth. Finally, at point P, the gel phase is solidified. This scheme was predicted from the observation of *Figure 2*; the lower parts in the gel phase have smaller pores, which grow into larger pores when the gel is solidified. In the final stage of pore growth, there should be almost no N6 contained in the pore parts. From the observation of the interface between the gel and solution in *Figure 2*, it is assumed that this membrane is formed according to the above process. A distinctive feature in the formation process of phase inversion membranes is liquid–liquid phase

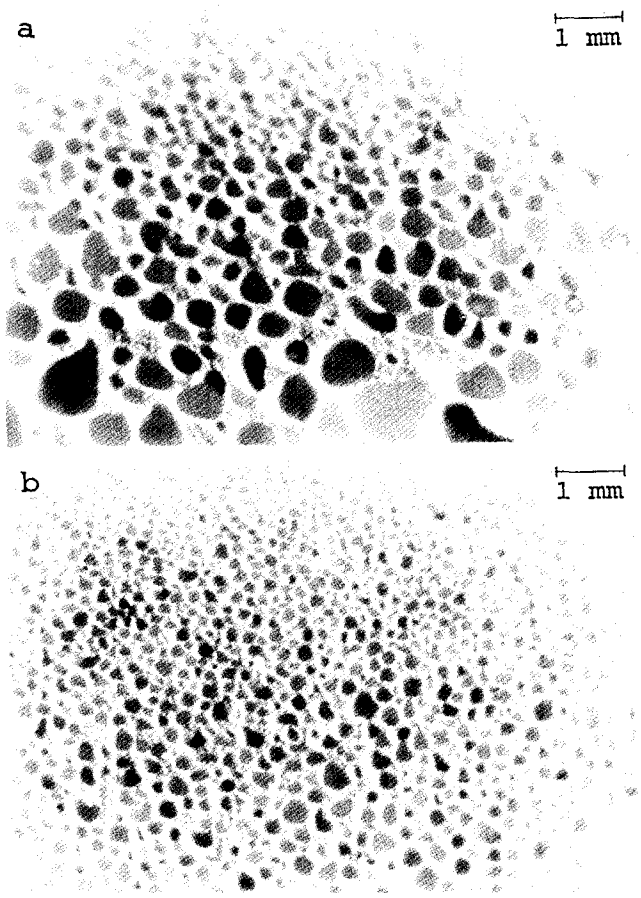

Figure 4 Morphology of vertical sections in the centre parts for N6 simulative membranes prepared from solutions of (a) 6.67 g and (b) 8.33 g N6/20 g $CaCl_2$/100 ml CH_3OH at 20°C

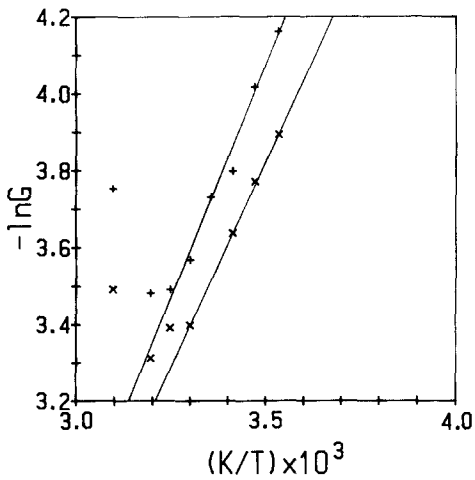

Figure 5 Relationship between $-\ln G$ and $1/T$ for sol–gel (×) and gel–solid (+) inversions in a solution of 6.67 g N6/20 g $CaCl_2$/100 ml CH_3OH. G is the gelation or solidification rate (cm h^{-1})

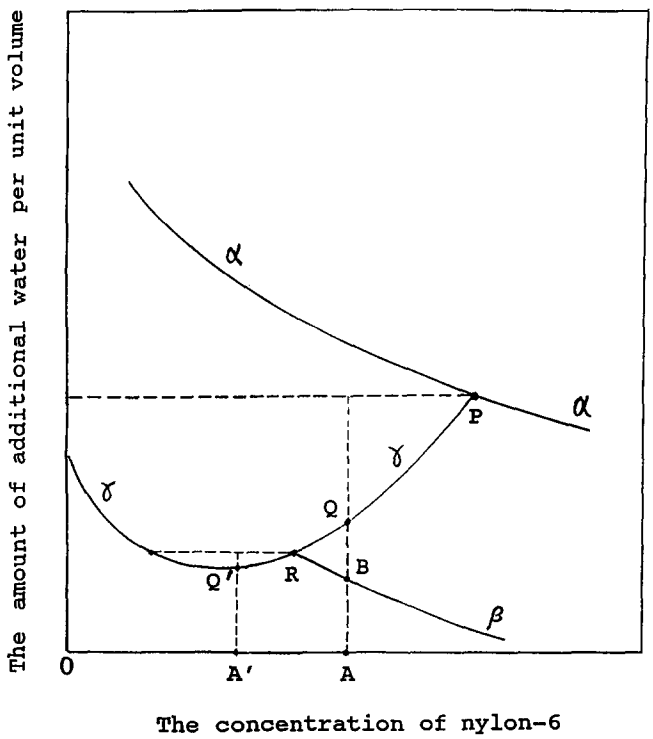

Figure 6 Schematic relationship between the concentration of N6 in a calcium chloride–methanol mixture and the amount of additional water per unit volume needed for solidification (α), sol–gel inversion (β) or phase separation (γ) at a horizontal cross-section point. The broken lines are supplementary ones

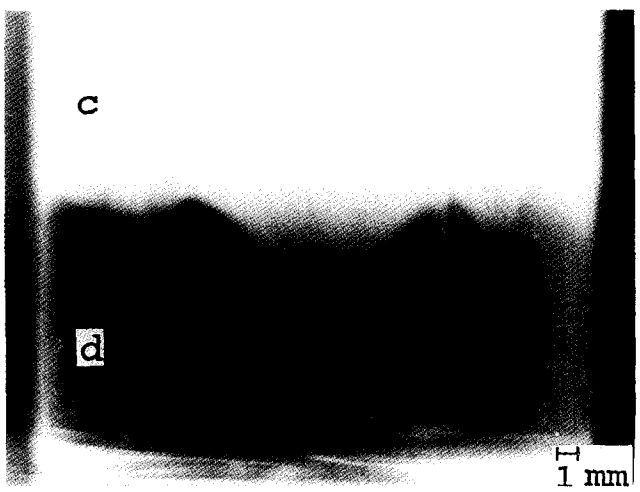

Figure 7 Photograph of gelation process for a solution of 6.67 g N6/20 g $CaCl_2$/100 ml CH_3OH in a room at about 20°C and 80% r.h.; (c) gel and (d) solution

separation before gelation[9]. With decreasing preparation temperature, it is assumed that, owing to the lowering of the solubility of N6 in the calcium chloride–methanol mixture, the curve α is shifted to the left (see *Figure 9*) and point P is moved to the left along the curve γ. Therefore, smaller pores should be formed as shown in *Figure 3*, because the pore size is determined principally by the amount of water added at point P. Kesting demonstrates[9] that the permeability of membranes increases monotonically with increasing non-solvent concentration in the casting solution. The permeability is related to the porosity of the

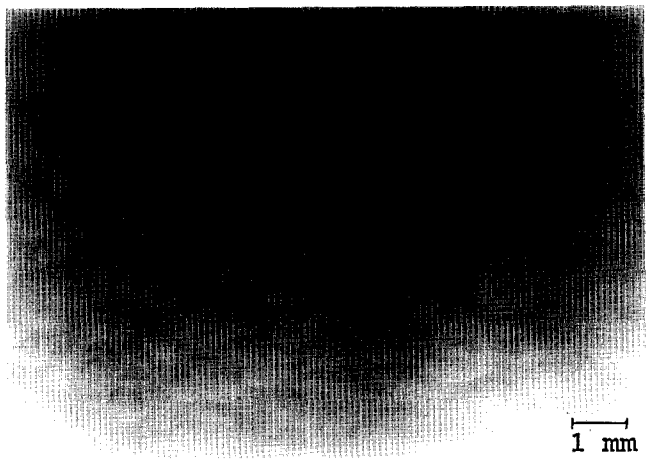

Figure 8 Photograph of phase separation in a gel. This picture was taken about a week after the photograph of *Figure 7*. At that time the whole solution had already gelled

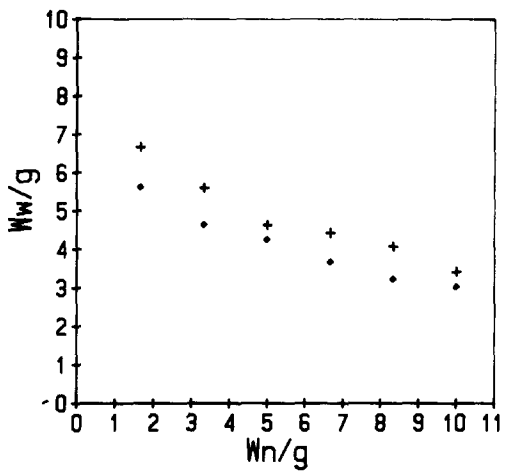

Figure 9 Relationship between the amount of additional water (W_w) needed for the solidification of N6 and the weight of N6 (W_n) per 20 g $CaCl_2$ for 10 g of a solution of 6.67 g N6/20 g $CaCl_2$/100 ml CH_3OH at 20°C (◆) and 30°C (+)

membranes[9]. Another process is predicted for a solution at point A in the range of the abscissa of curve β.

For a solution at point A. When the amount of water added crosses over a point B on the curve β, the solution is gelled and further increase of water into the region over point Q on the curve γ results in the phase separation structure of a gel and a liquid. The separated gel phase increases the concentration of N6 along the curve γ and the pores grow with increasing water. Finally at point P, the gel phase is solidified. This schematic process of pore formation could be expected for solutions of 8.33 and 10.0 g N6/20 g $CaCl_2$/100 ml CH_3OH, for which in the interface between solution and gel, liquid–liquid phase separation behaviour as shown in *Figure 2* was not observed clearly because the rate of diffusion of water into the solution is very low. *Figure 7* shows that gelation behaviour occurred naturally through moisture absorption and sufficient concentration for a solution of 6.67 g N6/20 g $CaCl_2$/100 ml CH_3OH in a room atmosphere at about 20°C and 80% r.h. At this stage, 12 days after the beginning of concentration, no phase separation behaviour was seen in

the gel phase by the naked eye. About a week after the photograph of *Figure 7* was taken, the whole solution had been converted to gel and the phase separation pattern as shown in *Figure 8* was observed. In turn, the gel phase changed to the solid with white colour very slowly from the top. If the degree of concentration is plotted as the abscissa in *Figure 6*, a pore formation process like this could also be applied to the schematic process from a solution at point A. The pore size should be smaller as the concentration of N6 in the casting solution or the degree of concentration is higher, because the arrival time from Q to P on curve γ, that is, the time of pore growth, becomes shorter.

Figure 9 shows the relationship between the amount of additional water (W_w) needed for the solidification of N6 and the weight of N6 (W_n) per 20 g $CaCl_2$ for 10 g of a solution of 6.67 g N6/20 g $CaCl_2$/100 ml CH_3OH at constant temperature (20 and 30°C). W_w decreased with increasing W_n. The curve α in *Figure 6* is predicted on the basis of this result.

ACKNOWLEDGEMENTS

The author wishes to thank Mr T. Suzuki *et al.* for helping in the experimental work, and Gunma University Foundation for Science and Technology for the support of travelling expenses to participate in the Europhysics Conference at Eindhoven in 1994.

REFERENCES

1 Takase, K. *Kobunshi* 1974, **23,** 592
2 Tanaka, N. *Sen-i Gakkaishi* 1986, **42,** T-431
3 Tanaka, N. and Hayashi, T. Preprint of China–Japan Bilateral Symposium on the Synthesis and Materials Science of Polymers (Beijing), 1984, p. 385
4 Tanaka, N. Proceedings of the International Symposium on Fiber Science and Technology (Hakone), 1985, p. 183
5 Tanaka, N. and Lin, J. *Sen-i Gakkaishi* 1988, **44,** 439
6 Nakajima, A. and Tanaami, K. *Polym. J.* 1973, **5,** 248
7 Tanaka, N. Preprint of Annual Meeting of Fiber Science and Technology (Tokyo), 1984, p. 198
8 Tanaka, N. Europhysics Conference Abstracts (Eindhoven), 1994, 18C, p. 38
9 Kesting, R. E. 'Synthetic Polymeric Membranes', Wiley, New York, 1985, p. 237
10 Kanzawa, J. and Katani, M. 'Porous Materials Handbook', CMC, Tokyo, 1988, pp. 210, 378
11 Manabe, S., Kamata, Y., Iijima, H. and Kamide, K. *Polym. J.* 1987, **19,** 391